NIH Public Access
Author Manuscript
Nat Med. Author manuscript; available in PMC 2012 March 19.

Published in final edited form as:
Nat Med. 2009 May ; 15(5): 572–576. doi:10.1038/nm.1919.

The Parametric Response Map: An Imaging Biomarker for Early Cancer Treatment Outcome

Craig J. Galbán[1], **Thomas L. Chenevert**[1], **Charles R. Meyer**[1], **Christina Tsien**[2], **Theodore S. Lawrence**[2], **Daniel A. Hamstra**[2], **Larry Junck**[3], **Pia C. Sundgren**[1], **Timothy D. Johnson**[4], **David J. Ross**[2], **Alnawaz Rehemtulla**[1,2], and **Brian D. Ross**[1]

[1]Department of Radiology, University of Michigan, Center for Molecular Imaging, Ann Arbor, Michigan 48109, USA

[2]Department of Radiation Oncology, University of Michigan, Center for Molecular Imaging, Ann Arbor, Michigan 48109, USA

[3]Department of Neurology, University of Michigan, Center for Molecular Imaging, Ann Arbor, Michigan 48109, USA

[4]Department of Biostatistics, University of Michigan, Center for Molecular Imaging, Ann Arbor, Michigan 48109, USA

Abstract

Here we describe the Parametric Response Map (PRM), a voxel-wise approach for image analysis and quantification of hemodynamic alterations during treatment for 44 patients with high-grade glioma. Relative cerebral blood volume (rCBV) and flow (rCBF) maps were acquired before treatment and after 1 and 3 weeks of therapy. We compared the standard approach using region-of-interest analysis for change in rCBV or rCBF to the change in perfusion parameters on the basis of PRM (PRM_{rCBV} and PRM_{rCBF}) for their accuracy in predicting overall survival. Neither the percentage change of rCBV or rCBF predicted survival, whereas the regional response evaluations based upon PRM were highly predictive of survival. Even when accounting for baseline rCBV, which is prognostic, PRM_{rCBV} proved more predictive of overall survival.

INTRODUCTION

Functional imaging approaches complement anatomical magnetic resonance imaging (MRI) scans and are increasingly being evaluated in oncology practice for diagnosis and assessment of treatment response[1–3]. Dynamic contrast-enhanced (DCE) and dynamic susceptibility-weighted contrast (DSC) MRI methods quantify a variety of hemodynamic parameters including microvessel permeability-surface area product, blood volume, and blood flow [4–9]. Several analyses techniques of the signal-time or concentration-time curves after contrast agent administration have been described, including the slope of the curve, the time to peak, the maximum peak enhancement, the wash out and the area under the curve (AUC) [10–13]. These descriptive parameters have been described for clinical applications, primarily tumor characterization. Relatively complicated pharmacokinetic modeling is

Corresponding Author: Brian D. Ross, Ph.D., Professor of Radiology, Co-Director, Center for Molecular Imaging, Biomedical Sciences Research Building, Room 2071, 109 Zina Pitcher Place, University of Michigan, Ann Arbor, MI 48109-2200, Phone: (734)-763-2099, Fax: (734)-763-5447, bdross@umich.edu.

COMPETING INTEREST STATEMENT

BDR, AR, CJG, CRM and TLC have a financial interest in the underlying technology. BDR and AR also have a financial interest in ImBio, LLC which has licensed the underlying PRM technology.

NIH-PA Author Manuscript
NIH-PA Author Manuscript
NIH-PA Author Manuscript

NIH-PA Author Manuscript

NIH-PA Author Manuscript

NIH-PA Author Manuscript

required to derive these physiological parameters, although the models tend to be based on simplifying assumptions and regimes where exchange of contrast material between the vascular space and interstitium is either flow limited or permeability limited[14,15]. This has led to the development of a diverse compilation of contrast agents for the purpose of increasing signal enhancement and blood pool localization, as well as numerous mathematical models for post-processing of the acquired data[16]. Nevertheless, a consensus has not been reached as to the optimal analytic approach for quantification of perfusion magnetic resonance changes as an early imaging biomarker of treatment response.

In this study, we obtained perfusion MRI data from a single-center prospective clinical trial in which individuals with grade III and IV gliomas were enrolled. To monitor for treatment-induced alterations of tumor microvasculature, perfusion magnetic resonance images were acquired prior to treatment and again 1 and 3 weeks after the start of therapy. We calculated hemodynamic parameter maps from dynamic susceptibility contrast images based on mathematical models to derive rCBV and rCBF maps for quantitative estimates of cerebral blood perfusion before and during treatment. We used the clinical data to compare two distinctly different post-processing analytical methods, one involving the currently used percent difference of the whole-tumor average (mean of the histogram), the other involving PRM, a new, voxel-wise analytical method (Fig. 1), for their predictive capabilities as imaging biomarkers for early assessment of treatment response. The comparison of the prognostic capability of the PRM approach with the traditional whole-tumor average method is presented. In addition, we compared the predictive value of PRM to baseline metrics (age and rCBV) which have been reported in a prospective studies to correlate with overall survival [17].

RESULTS

Patient Population

We included a total of 44 subjects with high-grade glioma (8 with a grade III glioma and 36 with a grade IV glioma, according to World Health Organization classifications) in this prospective study (see Supplementary Table 1). By Kaplan-Meier analysis the overall survival for the whole population was 12.8 months, with a one-year survival of 52.3%.

Comparison of PRM_{rCBV} and whole-tumor rCBV analysis

Results of rCBV analysis are presented for a representative patient with glioblastoma multiforme with overall survival of only 2.6 months from diagnosis (Fig. 2a–d). We observed contrast enhancement within the tumor before and 1 week after treatment (Fig. 2a). The distribution of rCBV values within the tumor before treatment had a mean of 2.0, which was unchanged at week 1 of therapy (Fig. 2b,c). However, at week 1 we observed substantial changes in PRM_{rCBV} voxels in the color overlay and scatter plot (Fig. 2d), which revealed that 17.2% of the tumor had increased blood volume (PRM_{rCBV+}) and 20.0% of the total tumor volume had decreased blood volume (PRM_{rCBV-}). We obtained similar results for PRM_{rCBF} at 1 week after treatment initiation and for both PRM_{rCBV} and PRM_{rCBF} at 3 weeks after treatment initiation (see Supplementary Figs. 1a–d and 2, respectively).

For comparison, we also studied a representative subject diagnosed with a glioblastoma multiforme who responded to therapy with overall survival of 20.4 months (Fig. 2e–h). We found that the mean rCBV values were also did not change significantly from before treatment initiation (rCBV=1.0) to 1 week after treatment initiation (Fig. 2f,g), and PRM_{rCBV} analysis also revealed negligible changes after 1 week of therapy (Fig. 2h). The corresponding scatter plot revealed that PRM_{rCBV+} and PRM_{rCBV-} changed by 3.4% and 4.3%, respectively (Fig. 2h). We obtained similar results for PRM_{rCBF} at 1 week after

NIH-PA Author Manuscript

NIH-PA Author Manuscript

NIH-PA Author Manuscript

treatment initiation and for both PRM_{rCBV} and PRM_{rCBF} at 3 weeks after treatment initiation (see Supplementary Figs. 1e–h and 3, respectively).

Correlation of image analysis with clinical outcomes

To correlate these early perfusion-based imaging biomarkers with overall survival, we used receiver operating characteristic (ROC) curve analysis to select for the optimized cutoffs by correlating each of the perfusion MRI parameters with the likelihood that the individual would be alive one year from diagnosis (23 of 44 individuals were alive at one year). The percentage change of rCBV and rCBF was not predictive of survival at one year when measured after 1 (Table 1) or 3 weeks (see Supplementary Table 2). However, when we assessed regional perfusion changes by PRM, the PRM_{rCBV-} was found to significantly predict survival at one year, with an AUC of 0.754 (p=0.004) and an optimal cutoff of 6.8% (Fig. 3a and Table 1). In comparison, the PRM_{rCBV+} and the percentage change of rCBV each generated AUC's of 0.528 and 0.557, respectively, neither of which are different from random chance (Table 1). We observed similar results for rCBF (Supplementary Table 2), and at week 3 both PRM metrics continued to be predictive of one-year survival, whereas the percentage change in rCBV and rCBF were not (Supplementary Fig. 3 and Supplementary Table 2).

When we assessed PRM metrics with a long-rank test and with Cox-proportional hazards models as continuous variables (data not shown), there were indirect correlations between overall survival and both PRM_{rCBV-} and PRM_{rCBF-} at both 1 and 3 weeks after treatment initiation (see Supplementary Fig. 4 and Supplementary Table 2). Subjects whose tumors maintained their pre-treatment tumor blood volume after 1 week of therapy (that is, low PRM_{rCBV-}, Fig. 3b and Table 1) lived longer (20.4 months) as compared to those who showed a larger portion of their tumor with a decrease in blood volume in response to therapy (10.2 months, p=0.009). We obtained similar results for PRM_{rCBF-} (Supplementary Fig. 4d). In addition, PRM_{rCBV-} and PRM_{rCBF-} after 3 weeks of treatment both resulted in a significant correlation with overall survival ($P = 0.009$ and $P = 0.028$), even when the population was stratified using optimal cutoffs obtained from week 1 data (Supplementary Fig. 4e,f and Supplementary Table 2).

Baseline tumor perfusion has recently been shown to be prognostic for predicting time to progression in subjects with glioma[17]. Therefore, to determine whether measured changes in tumor perfusion in response to treatment would add further to clinical evaluation, we analyzed the impact of baseline subject characteristics as well as perfusion characteristics in response to treatment at one week. In this population, age and baseline tumor perfusion ($rCBV_0$) were strongly predictive of overall survival by log-rank test ($p<0.02$ and $p<0.001$, respectively). On the basis of ROC analysis for one year survival, we found $rCBV_0$ ($p<0.001$) to be a more robust predictor for survival than $rCBF_0$ (p=0.046); therefore, we focused on a multivariate model incorporating age, $rCBV_0$ and PRM_{rCBV-}. Notably, univariate analysis using a binary logistic regression revealed that all three of these parameters (Age, $rCBV_0$, and PRM_{rCBV-}) correlated with one year survival (Table 2). However, multivariate analysis revealed that both subject age (<50 vs. 50+) and PRM_{rCBV-} (≤6.8% vs. >6.8%) were predictive of survival, whereas $rCBV_0$ (≤1.85 vs. >1.85) was not (Table 2).

DISCUSSION

Previous studies investigating perfusion MRI for tumor diagnosis and response monitoring have evaluated the capabilities of different types of contrast agents[16], magnetic resonance sequences or outcome parameters (descriptive and quantitative) as potential biomarkers[14]. These studies have historically relied on the whole-tumor mean value as the summary

NIH-PA Author Manuscript

NIH-PA Author Manuscript

NIH-PA Author Manuscript

statistic of the perfusion maps for quantification of hemodynamic parameters, with varying success[18,19]. Here we observed quantitative alterations in rCBV and rCBF maps after therapy for some individuals during treatment. However, the average change in mean tumor perfusion during treatment was found to lack sufficient sensitivity to provide an accurate prediction of treatment outcome. This was probably the result of the varying changes in blood volume or flow (both increasing and decreasing) occurring throughout the tumor, which ultimately desensitizes the whole tumor measurement. The minimal percentage changes in the rCBV or rCBF observed in this study further support this contention. In comparison, spatial information is preserved when using the PRM approach, and local variations in terms of increased, decreased and unchanged tumor PRM voxels after therapy can be delineated from each other and, therefore, quantified and visualized within the context of the anatomical image. As shown for the therapeutically non-responsive subject, PRM_{rCBV} revealed a large number of voxels in which rCBV values increased (PRM_{rCBV+}) and decreased (PRM_{rCBV-}) within the tumor volume. In contrast, in the therapeutically responsive subject, PRM_{rCBV} analysis did detect changes in PRM_{rCBV+} and PRM_{rCBV-} at week 1, although overall changes were found to be relatively small. In instances of spatially-varying heterogeneous response, sub-regions were found to increase in rCBV, whereas other regions to decrease in rCBV, resulting in the attenuation of detectable change in the whole-tumor mean statistic. However, PRM was a more sensitive method for quantification of treatment-induced alterations in rCBV values, as portions of the tumor with increasing and decreasing values were considered as separate measures. Analysis of the prognostic capabilities of both PRM and percentage change of rCBV and rCBF for early assessment of treatment response was accomplished. The percent change in rCBV was not able to provide sufficient sensitivity or specificity for stratification of responding from non-responding subjects at the 1 week time interval. In contrast, PRM_{rCBV-} was found to be highly predictive of overall survival. Similar results from rCBV analyses were observed for rCBF.

Quantification of treatment response by region of interest (ROI)-based mean parameters did not provide a substantial early treatment response prognostic outcome; however, the quantifiable hemodynamic parameter found most predictive of overall survival was based upon the volume fraction of the tumor associated with decreasing rCBV or rCBF values. Early stratification of responding from non-responding subjects worked equally well for both PRM_{rCBV-} and PRM_{rCBF-} at 1 week after treatment initiation. This trend continued into week 3 after treatment initiation. The prognostic importance of changes in perfusion as quantified by PRM_{rCBV} was retained even when baseline individual age and rCBV were taken into account, which have previously been shown to be prognostic in subjects with high-grade glioma[17]. In addition to these imaging-based biomarkers, molecular and histological markers have a growing role in oncology in general, including the treatment of subjects with brain tumors. Future efforts investigating combinations of biomarkers may provide for improved prognostic accuracy (Supplementary Discussion).

Overall, the observation that decreases in tumor blood volume or flow as measured by PRM as early as 1 week into treatment are prognostic for overall survival in individuals with grade III and IV gliomas is noteworthy. It is possible that a rapid reduction in local blood flow or volume which occurs during radiation treatment may portend a worse response to therapy, perhaps owing to development of regional acute hypoxia and radiation resistance. In support of this, recent literature has shown that maintaining or improving tumor microvasculature was a strong predictor of individual outcome during therapy[3]. An increase in PRM_{rCBV+} may be the result of an increase in overall microvessel density or a dilation of vessel diameter, as both could result in a net increase in tumor blood volume and flow. These processes may require additional time to fully develop, lagging behind hypoxic-induced events that are suspected to govern PRM_{rCBV-}, therefore negating any early predictive value in PRM_{rCBV+}. However, the observations made here in regard to regional changes in blood

NIH-PA Author Manuscript

NIH-PA Author Manuscript

NIH-PA Author Manuscript

flow and volume through the approach provided by PRM analysis are hypothesis-generating only and do not necessarily reflect a causal impact upon treatment efficacy but do suggest further areas of inquiry.

In this study, we presented PRM as a new voxel-wise method for analyzing perfusion maps to assess early tumor treatment response. Although registration-based voxel-by-voxel scatter plot change analysis has been used to quantify diffusion MRI parameters [20–24], this is the first time it has been investigated in the context of perfusion MRI. The PRM approach used both rCBV and rCBF maps of tumors before therapy and at early intratreatment intervals to provide for voxel-wise quantification and visualization of local treatment-induced alterations in tumor hemodynamics in subjects with grade III and IV gliomas. The ability of PRM to maintain the spatial information on a voxel-by-voxel basis provided the ability to detect and quantify local hemodynamic alterations within the tumor. Although the need for image registration, which may introduce error if large changes in tumor volume occur between interval exams may be considered a limitation, the present study clearly shows the ability of this technique to predict overall survival in a cohort of subjects with grade III and IV gliomas (Supplementary Discussion). In addition, PRM continued to generate significant results even if changes of up to 50% in the optimal cutoff were used (Supplementary Discussion). The PRM imaging biomarker provides the ability to quantify the various components of tumor hemodynamic heterogeneity during treatment with the sensitivity necessary for early prediction of subject response. This is especially compelling, as new antiangiogenic and antivascular therapies are under active development and are beginning to have a considerable impact on patient care [25–30].

Finally, PRM can be applied to the analysis of a variety of perfusion MRI parameters such as vascular permeability (preliminary results shown in Supplementary Figs. 5 and 6) and extravascular leakage space. Extension of PRM for analysis of other clinical imaging modalities (such as perfusion computed tomography, positron emission tomography and single-photon emission computed tomography) should be feasible, thus providing for a possible unified analytical approach for quantitative image analysis for early prediction of tumor therapeutic response.

METHODS

Subjects

Subjects with pathologically proven grade III and IV gliomas were enrolled on a protocol of intra-treatment MRI. We obtained informed consent, and images and medical record use was approved by the University of Michigan Institutional Review Board. We evaluated 44 individuals before therapy and 1 and 3 weeks after treatment initiation.

We delivered radiotherapy by three-dimensional-conformal therapy or intensity-modulated radiation therapy with 6 MV or greater photons. We used standard techniques with a 2.0–2.5 cm margin on either the enhancing region on gadolinium-enhanced scans or the abnormal signal on T_2-weighted scans to 46–50 Gy, with the central gross tumor treated to a final median dose of 70 Gy in 6–7 weeks [31]. We treated 24 of these individuals on a phase 2 protocol of high-dose (>60 Gy) radiation therapy concurrent with temozolamide. We commonly used chemotherapy and delivered it as necessary according to clinical circumstances (Supplementary Table 1).

Magnetic resonance imaging scans

We performed MRI scans 1 week before and 1 and 3 weeks after the start of radiation. We acquired images on either a 1.5T Signa (General Electric Medical Systems) (n = 30 subjects) or 3T Achieva (Philips Medical Systems) (n = 14 subjects) system. For DSC imaging, we

NIH-PA Author Manuscript

NIH-PA Author Manuscript

NIH-PA Author Manuscript

acquired 14–20 slices by a gradient-echo echo-planar imaging pulse sequence (TR=1.5 to 2s, TE=50 to 60ms, field of view 220×220 mm^2, matrix 128×128, flip angle 60°, and 4 to 6mm thickness and 0mm gap). We intravenously injected gadolinium-diethylenetriamine pentaacetic acid (Gd-DTPA; Bayer HealthCare Pharmaceuticals) as a bolus through a power injector at a rate of 2 mL s^{-1}, followed immediately by 15 ml of saline flush at the same rate. Subsequently, we acquired gadolinium-enhanced T_1-weighted imaging.

We generated CBV and CBF maps from DSC images as described previously [3]. To assess differences in tumor blood volume and flow during treatment and between subjects, we normalized CBV and CBF maps to values within white matter regions contralateral to the tumor to generate relative rCBV and rCBF maps. For normalization, we used those white matter ROIs that were contralateral to tumor, had received <30 Gy accumulated dose and were as large as possible while still avoiding regions with susceptibility artifacts and partial volume averaging.

Image Analysis

We co-registered rCBV and rCBF maps before and after treatment to gadolinium-enhanced T_1-weighted images acquired before treatement using mutual information as an objective function and simplex as an optimizer [32]. The co-registration of different and similar-weighted MRI scans for the same subject is totally automatic and assumes a rigid-body geometry relationship, that is, rotation and translation, between head scans. After co-registration, brain tumors, manually contoured by a neuroradiologist, were defined within the enhancing regions of the tumor on the gadolinium-enhanced T_1-weighted images. Shrinkage or growth of the tumor during the time between scans may have occurred; therefore, only voxels that were present in both before treatment and intratreatment tumor volumes were included. Subsequent to co-registration, the resultant maps consist of spatially aligned voxels with rCBV and rCBF values prior and 1 or 3 weeks after treatment initiation.

We determined the PRM_{rCBV} by first calculating the difference between the rCBV (ΔrCBV = intratreatment rCBV − pretreatment rCBV) for each voxel within the tumor before therapy and at week 1 and 3 post-treatment initiation. We designated the voxels yielding ΔrCBV greater than a predetermined threshold set to 1.2 (details described below) as red. Blue voxels represent volumes whose rCBV decreased by more than 1.2, and the green voxels represent voxels within the tumor that were unchanged (that is, the absolute value of ΔrCBV was ≤ 1.2). The volume fractions within the tumor determined from PRM_{rCBV} were PRM_{rCBV+} (increasing rCBV), PRM_{rCBV-} (decreasing rCBV), and PRM_{rCBV0} (unchanged rCBV). We empirically calculated the thresholds that designate a significant change in rCBV within a voxel from seven randomly selected individuals. For each subject, we used a region of interest within the contralateral brain containing normal gray and white matter was used to acquire a range of rCBV before and one week after therapy initiation. Combining the data from all seven subjects, we performed linear least squares regression analysis on the pre-treatment and intratreatment rCBV values. We then determined the 95% confidence intervals from the resulting linear least squares analysis. After the PRM_{rCBV} analysis, we calculated the percent difference of the mean rCBV ($\%rCBV_{ROI}=100\times[rCBV_{post\text{-}RT}-rCBV_{pre\text{-}RT}]\cdot rCBV_{pre\text{-}RT}^{-1}$) over the tumor volume and compared to PRM_{rCBV} results. We used the same procedure for determining the thresholds (±2.1) and PRM of rCBF maps. We used the thresholds determined from week 1 data for PRM analyses of rCBV and rCBF at week 3 after treatment initiation.

Statistical Analysis

We performed ROC curve analysis for correlation of the representative imaging parameters with subject survival one year from diagnosis. We obtainted the AUC to distinguish which

NIH-PA Author Manuscript

NIH-PA Author Manuscript

NIH-PA Author Manuscript

continuous variables (PRM and percentage change of perfusion parameter (rCBV and rCBF)) were predictive measures of outcome. For parameters acquired 1 week after treatment initiation that were statistically significant predictors of survival, we selected cutoffs from ROC curves on the basis of optimal values of sensitivity and specificity. We then stratified the population on the basis of the ROC cutoffs and assessed overall survival using the log-rank test and Kaplan-Meier survival curves. We did the same analysis was on 3 week PRM and whole-tumor data, except we used the optimal cutoffs from 1 week data for stratification. We correlated PRM, a treatment response measure, and both age and baseline rCBV, which have known prognostic value, to one year survival following diagnosis by univariate and multivariate binary logistic regression. We made all statistical computations with a statistical software package (SPSS Software Products), and we declared results statistically significant at the two-sided 5% comparison-wise significance level ($p < 0.05$).

Supplementary Material

Refer to Web version on PubMed Central for supplementary material.

Acknowledgments

This work was supported by the National Institutes of Health Research Grants P01CA85878, R24CA83099 and P50CA093990.

References

1. O'Connor JP, Jackson A, Parker GJ, Jayson GC. DCE-MRI biomarkers in the clinical evaluation of antiangiogenic and vascular disrupting agents. Br J Cancer. 2007; 96:189–195. [PubMed: 17211479]
2. Zahra MA, Hollingsworth KG, Sala E, Lomas DJ, Tan LT. Dynamic contrast-enhanced MRI as a predictor of tumour response to radiotherapy. Lancet Oncol. 2007; 8:63–74. [PubMed: 17196512]
3. Cao Y, et al. Clinical investigation survival prediction in high-grade gliomas by MRI perfusion before and during early stage of RT. Int J Radiat Oncol Biol Phys. 2006; 64:876–885. [PubMed: 16298499]
4. Ostergaard L, Weisskoff RM, Chesler DA, Gyldensted C, Rosen BR. High resolution measurement of cerebral blood flow using intravascular tracer bolus passages. Part I: Mathematical approach and statistical analysis. Magn Reson Med. 1996; 36:715–725. [PubMed: 8916022]
5. Rosen BR, Belliveau JW, Vevea JM, Brady TJ. Perfusion imaging with NMR contrast agents. Magn Reson Med. 1990; 14:249–265. [PubMed: 2345506]
6. Brix G, et al. Microcirculation and microvasculature in breast tumors: pharmacokinetic analysis of dynamic MR image series. Magn Reson Med. 2004; 52:420–429. [PubMed: 15282828]
7. Hoffmann U, Brix G, Knopp MV, Hess T, Lorenz WJ. Pharmacokinetic mapping of the breast: a new method for dynamic MR mammography. Magn Reson Med. 1995; 33:506–514. [PubMed: 7776881]
8. Tofts PS. Modeling tracer kinetics in dynamic Gd-DTPA MR imaging. J Magn Reson Imaging. 1997; 7:91–101. [PubMed: 9039598]
9. Degani H, Gusis V, Weinstein D, Fields S, Strano S. Mapping pathophysiological features of breast tumors by MRI at high spatial resolution. Nat Med. 1997; 3:780–782. [PubMed: 9212107]
10. Galbraith SM, et al. Reproducibility of dynamic contrast-enhanced MRI in human muscle and tumours: comparison of quantitative and semi-quantitative analysis. NMR Biomed. 2002; 15:132–142. [PubMed: 11870909]
11. Hylton N. Dynamic contrast-enhanced magnetic resonance imaging as an imaging biomarker. J Clin Oncol. 2006; 24:3293–3298. [PubMed: 16829653]

NIH-PA Author Manuscript

NIH-PA Author Manuscript

NIH-PA Author Manuscript

12. Thomas AL, et al. Phase I study of the safety, tolerability, pharmacokinetics, and pharmacodynamics of PTK787/ZK 222584 administered twice daily in patients with advanced cancer. J Clin Oncol. 2005; 23:4162–4171. [PubMed: 15867205]
13. Xiong HQ, et al. A phase I surrogate endpoint study of SU6668 in patients with solid tumors. Invest New Drugs. 2004; 22:459–466. [PubMed: 15292716]
14. Tofts PS, et al. Estimating kinetic parameters from dynamic contrast-enhanced T(1)-weighted MRI of a diffusable tracer: standardized quantities and symbols. J Magn Reson Imaging. 1999; 10:223–232. [PubMed: 10508281]
15. Eyal E, Degani H. Model-based and model-free parametric analysis of breast dynamic-contrast-enhanced MRI. NMR Biomed. 2007
16. Kiessling F, Morgenstern B, Zhang C. Contrast agents and applications to assess tumor angiogenesis in vivo by magnetic resonance imaging. Curr Med Chem. 2007; 14:77–91. [PubMed: 17266569]
17. Law M, et al. Gliomas: predicting time to progression or survival with cerebral blood volume measurements at dynamic susceptibility-weighted contrast-enhanced perfusion MR imaging. Radiology. 2008; 247:490–498. [PubMed: 18349315]
18. Law M, Young R, Babb J, Pollack E, Johnson G. Histogram analysis versus region of interest analysis of dynamic susceptibility contrast perfusion MR imaging data in the grading of cerebral gliomas. AJNR Am J Neuroradiol. 2007; 28:761–766. [PubMed: 17416835]
19. Young R, Babb J, Law M, Pollack E, Johnson G. Comparison of region-of-interest analysis with three different histogram analysis methods in the determination of perfusion metrics in patients with brain gliomas. J Magn Reson Imaging. 2007; 26:1053–1063. [PubMed: 17896374]
20. Hamstra DA, et al. Evaluation of the functional diffusion map as an early biomarker of time-to-progression and overall survival in high-grade glioma. Proc Natl Acad Sci U S A. 2005; 102:16759–16764. [PubMed: 16267128]
21. Lee KC, et al. A feasibility study evaluating the functional diffusion map as a predictive imaging biomarker for detection of treatment response in a patient with metastatic prostate cancer to the bone. Neoplasia. 2007; 9:1003–1011. [PubMed: 18084607]
22. Lee KC, et al. An Imaging Biomarker of Early Treatment Response in Prostate Cancer that Has Metastasized to the Bone. Cancer Res. 2007; 67:3524–3528. [PubMed: 17440058]
23. Moffat BA, et al. Functional diffusion map: a noninvasive MRI biomarker for early stratification of clinical brain tumor response. Proc Natl Acad Sci U S A. 2005; 102:5524–5529. [PubMed: 15805192]
24. Moffat BA, et al. The functional diffusion map: an imaging biomarker for the early prediction of cancer treatment outcome. Neoplasia. 2006; 8:259–267. [PubMed: 16756718]
25. Liu G, et al. Dynamic contrast-enhanced magnetic resonance imaging as a pharmacodynamic measure of response after acute dosing of AG-013736, an oral angiogenesis inhibitor, in patients with advanced solid tumors: results from a phase I study. J Clin Oncol. 2005; 23:5464–5473. [PubMed: 16027440]
26. Morgan B, et al. Dynamic contrast-enhanced magnetic resonance imaging as a biomarker for the pharmacological response of PTK787/ZK 222584, an inhibitor of the vascular endothelial growth factor receptor tyrosine kinases, in patients with advanced colorectal cancer and liver metastases: results from two phase I studies. J Clin Oncol. 2003; 21:3955–3964. [PubMed: 14517187]
27. Mross K, et al. Phase I clinical and pharmacokinetic study of PTK/ZK, a multiple VEGF receptor inhibitor, in patients with liver metastases from solid tumours. Eur J Cancer. 2005; 41:1291–1299. [PubMed: 15939265]
28. O'Donnell A, et al. A Phase I study of the angiogenesis inhibitor SU5416 (semaxanib) in solid tumours, incorporating dynamic contrast MR pharmacodynamic end points. Br J Cancer. 2005; 93:876–883. [PubMed: 16222321]
29. Rugo HS, et al. Phase I trial of the oral antiangiogenesis agent AG-013736 in patients with advanced solid tumors: pharmacokinetic and clinical results. J Clin Oncol. 2005; 23:5474–5483. [PubMed: 16027439]

NIH-PA Author Manuscript

NIH-PA Author Manuscript

NIH-PA Author Manuscript

30. Wedam SB, et al. Antiangiogenic and antitumor effects of bevacizumab in patients with inflammatory and locally advanced breast cancer. J Clin Oncol. 2006; 24:769–777. [PubMed: 16391297]

31. Chan JL, et al. Survival and failure patterns of high-grade gliomas after three-dimensional conformal radiotherapy. J Clin Oncol. 2002; 20:1635–1642. [PubMed: 11896114]

32. Meyer CR, et al. Demonstration of accuracy and clinical versatility of mutual information for automatic multimodality image fusion using affine and thin-plate spline warped geometric deformations. Med Image Anal. 1997; 1:195–206. [PubMed: 9873906]

NIH-PA Author Manuscript
NIH-PA Author Manuscript
NIH-PA Author Manuscript

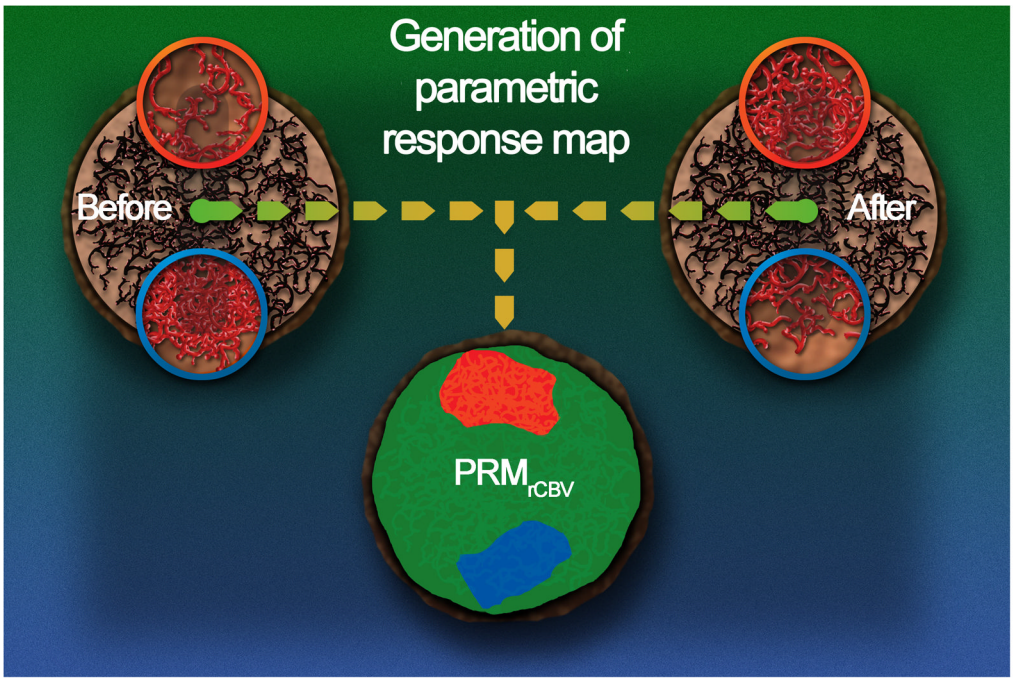

Figure 1.

PRM is a fundamentally distinct approach from the region of interest method in that it retains spatial alterations in perfusion values early following treatment initiation. This quantification method relies upon a voxel-by-voxel comparison of perfusion maps through image co-registration of pre-treatment images with those obtained at short time intervals following treatment initiation in an effort to provide early assessment of treatment outcome. As illustrated in this figure, the tumor environment may have three local hemodynamic outcomes throughout the course of therapy. An increase in rCBV above a specified threshold suggests a significant increase in the microvascular density or enlargement of blood vessel diameter (i.e. blood volume) within the tumor, in which case these voxels would be color coded red in the PRM analysis approach applied to rCBV (PRM_{rCBV}). Alternatively, treatment may result in a significant reduction in rCBV within the tumor in which case voxels within those regions would be coded blue. Voxels in regions which were relatively unaffected by therapy would be coded green. The PRM_{rCBV} analysis retains the spatial rCBV information as coded by color overlay on anatomic Gd-enhanced T_1-weighted images and also quantification of the total number of tumor voxels (on a percentage of total tumor volume) which exhibited an increase (red: PRM_{rCBV+}), decrease (blue: PRM_{rCBV-}) or unchanged (green: PRM_{rCBV0}) rCBV values using scatter plot analysis. This quantification of spatially altered rCBV values provided the opportunity to evaluate the PRM approach as a prognostic imaging biomarker for early treatment response assessment through correlation with overall survival.

NIH-PA Author Manuscript

NIH-PA Author Manuscript

NIH-PA Author Manuscript

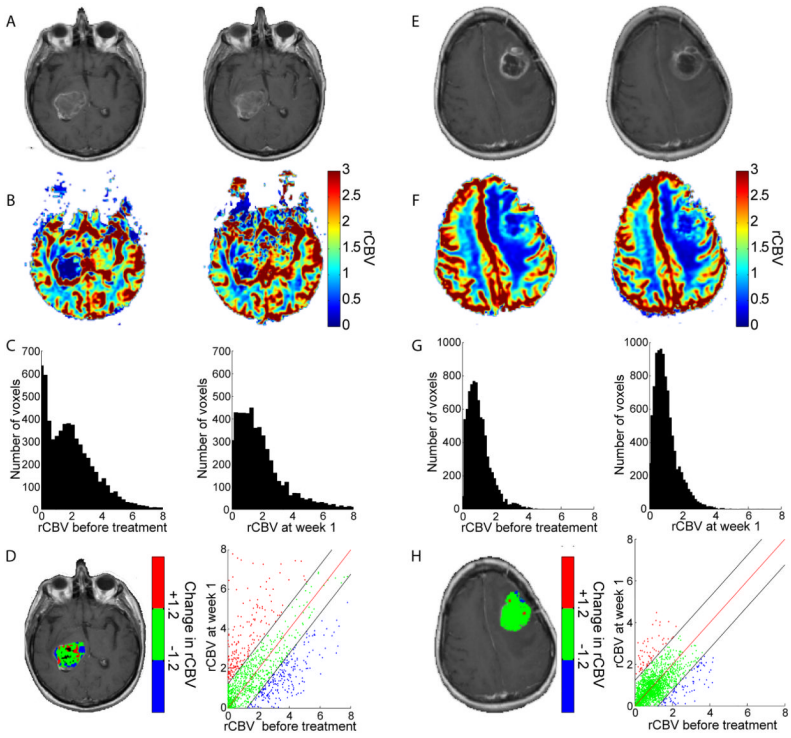

Figure 2.

Individuals with a glioblastoma multiforme designated by PRM_{rCBV-} stratification as a non-responder (**a–d**; survival time of 2.9 months) and responder (**e–h**; survival time of 20.4 months). (**a,e**) Gd-enhanced T_1-weighted MR images, (**b,f**) rCBV with color scale and (**c,g**) rCBV histograms of tumor, at 0 (left panels) and 1 (right panels) week post-therapy. Representative slices of (**d,h**) PRM_{rCBV} color-coded ROI superimposed onto a Gd-enhanced T_1-weighted MR image pre-therapy and scatter plot showing the distribution of rCBV pre and post-therapy for the entire 3-dimensional tumor volume. Unity and 95% confidence intervals within the scatter plot are designated by a red and two black lines, respectively. Voxels with significantly increasing, decreasing or unchanged rCBV are designated by red, blue and green dots. Voxels in which the perfusion model had generated erroneous results were colored black on the PRM overlay and were not included in the whole-tumor or PRM analyses.

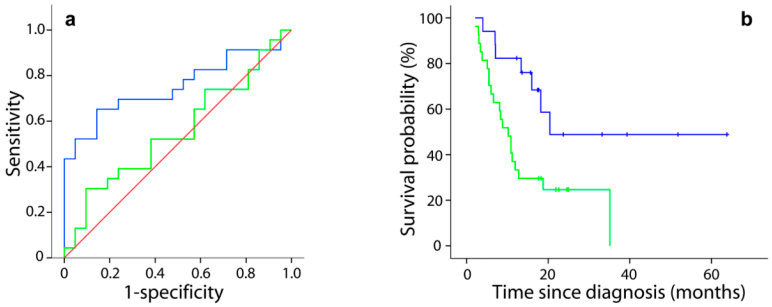

Figure 3.

(**a**) ROC curves for PRM_{rCBV-} (blue line) and percentage change of rCBV (green line) at week 1 post-treatment. (**b**) Kaplan-Meier survival plots for overall survival are presented as a function of PRM_{rCBV-} stratification at weeks 1 post-treatment initiation. Blue lines indicates $PRM_{rCBV-} \leq$ cutoff and green lines indicates $PRM_{rCBV-} >$ cutoff.

NIH-PA Author Manuscript
NIH-PA Author Manuscript
NIH-PA Author Manuscript

NIH-PA Author Manuscript
NIH-PA Author Manuscript
NIH-PA Author Manuscript

Table 1

ROC and Survival Analysis Results at Week 1

Parameter	AUC	Responders Median Survival (n)	Non-Responders Median survival (n)	p value
PRM_{rCBV-}	0.754 (p=0.004)	20.4 (17)	10.2 (27)	0.009
$\%rCBV_{ROI}$	0.557	–	–	–

Area under the curve (AUC) and significant p values were generated from the ROC analysis of PRM_{rCBV-} and the percent change in rCBV ($\%rCBV_{ROI}$). The optimal cutoffs at week 1, determined by ROC analysis, were used for the Kaplan-Meier analysis. Median survival, non-responders (≤ cutoff) and responders (> cutoff), and group populations (in parentheses) were presented for significant results (p values) generated from Kaplan-Meier and log-rank test. Statistical significance was assessed at $p<0.05$.

NIH-PA Author Manuscript

NIH-PA Author Manuscript

NIH-PA Author Manuscript

Table 2

Binary Logistic Regression (p values)

Parameter	Univariate (p value)	Multivariate (p value)
Age*	0.008	0.011
$rCBV_0$*	0.001	0.151
PRM_{rCBV}†	0.003	0.019

Binary logistic regression was performed to determine the correlation of age, baseline rCBV ($rCBV_0$) and PRM_{rCBV} to one year survival. Stratification of subject population was 50 years for age, 1.8 for $rCBV_0$ or 6.8 for PRM_{rCBV}. Results are presented for univariate and multivariate (all three parameters) regressions.

*Pre-Treatment Measurement;

†Response Measurement.